

# Initial insight to effect of exercise on maximum pressure in the left ventricle using 2D fluid-structure interaction model

Arezoo khosravi<sup>1\*</sup>, Hamidreza Ghasemi Bahraseman<sup>2</sup>, Davood Kazemi-Saleh<sup>1</sup>

<sup>1</sup> Atherosclerosis research center, Tehran, Iran.

<sup>2</sup> Department of Biomechanics, Science and Research Branch, Islamic Azad University, Tehran, Iran.

**Aims:** Study of maximum pressure in the left ventricle (MPLV) has already been a challenging aspect of clinical diagnosis. The aim of this study was to propose a model to estimate the MPLV for a healthy subject based on cardiac outputs measured by echo-Doppler (non-invasive) and catheterization (invasive) techniques at rest and during exercise.

**Study design and methodology:**

Blood flow through the aortic valve was measured by Doppler flow echocardiography. The aortic valve geometry was then calculated by echocardiographic imaging. A Fluid-Structure Interaction (FSI) simulation was performed, using an Arbitrary Lagrangian-Eulerian (ALE) mesh. Boundary conditions were defined as pressure loads on ventricular and aortic sides during ejection phase. The FSI modelling was applied to determine a numerical relationship between the cardiac output to left ventricular and aortic diastolic pressures. These relationships enable the prediction of pressure loads from cardiac outputs measured by invasive and non-invasive clinical methods.

**Results:** Peak ventricular systolic pressure calculated from cardiac output of Doppler method, Fick oximetric and Thermodilution methods led to a 82.1%, 95.6% and 147% increment throughout exercise, respectively. The mean slopes obtained from curves of ventricular systolic pressure based on Doppler, Fick oximetric and Thermodilution methods are 1.27, 1.85 and 2.65 mmHg.min, respectively. Our predicted Fick-MPLV values were 8% to 19% lower, 17% to 25% lower for Thermodilution-MPLV, and 57% to 73% lower for Doppler-MPLV values when compared to clinical reports.

**Conclusion:** Predicted results are in good agreement with values in the literature. The method, however, requires validation by additional experiments, comprising independent quantifications of MPLV. Since flow depends on the pressure loads, measuring more accurate intraventricular pressures helps to understand the cardiac flow dynamics for better clinical diagnosis. Furthermore, the method is noninvasive, safe, cheap and practical. As clinical Fick-measured values have been known to be more accurate, our Fick-based prediction could be the most applicable.

**Keywords:** Fluid-Solid interaction, Fick oximetric, maximum pressure in the left ventricle, Thermodilution.

## 22 1. INTRODUCTION

23

24 Cardiac disease is a major cause of death in industrialized countries, in spite of advances in  
25 prevention, diagnosis, and therapy [1]. Despite challenging aspects of clinical diagnosis, the  
26 investigation of maximum pressure in the left ventricle (MPLV) assessment is among the  
27 most clinically important [2]. Therefore, detecting MPLV during blood pumping is important  
28 for recognition of such diseases. This study has used a Fluid-Structure Interaction (FSI)  
29 model to predict MPLV and trans-aortic pressure. Common invasive techniques like Fick  
30 oximetric and Thermodilution have associated risks [4]. MPLV measurements were first  
31 examined using invasive catheters [5]. Brenner et al. studied the MPLV at peak pressure  
32 which was estimated in five infants using echo-Doppler and catheterisation [6]. Greenberg et  
33 al. introduced a method to evaluate the MPLV by analyzing intraventricular flow velocities  
34 [7]. Firstenberg et al [8] and Tonti et al [9] non-invasively determined correlations between  
35 the earlier invasive MPLV measurements. Few studies have estimated MPLV with respect  
36 to the heart rate variations during exercise. However, heart rate changes during exercise,  
37 simultaneous intraventricular pressure gradients and ejection flow patterns have been  
38 measured by a multisensor catheter at rest and exercise [10]. Redaelli and Montevecchi  
39 studied only intraventricular pressure gradients using fluid structure interaction at a heart  
40 rate of 72 bpm. Without using an exercise protocol [11] Clavin et al and Spinelli et al used  
41 an electrical model to assess cardiac function based on left intraventricular-impedance at  
42 rest condition [12, 13].

43 Experimentally, intraventricular pressure is a valuable measurement. Nonetheless, due to  
44 the fact that the heart is not perfused via the normal route, intraventricular pressure cannot  
45 be measured even with sophisticated medical instruments like an open-ended catheter [14].  
46 These studies demonstrated the importance of pressure measurements to be certain of  
47 efficient LV performances.

48 FSI simulations are overall well matched to cardiovascular modeling [15, 16]. This method  
49 requires the use of an Arbitrary Lagrange-Euler (ALE) mesh to analyze both structural  
50 deformation and fluid flow; i.e. Computational Fluid Dynamics and Finite Element Analysis  
51 [17, 18]. Recently, FSI has been used to investigate heart valves [19, 20, 21, 22, 23, 24  
52, 25, 26]. Previously we have measured the cardiac output and stroke volume for a healthy  
53 subject by coupling an echo-Doppler method with an FSI simulation at rest and during  
54 exercise and particular attention was given to validating the model versus measures of  
55 cardiac function that could be calculated by applying clinical protocols, with varying exercise  
56 [27] and the effect of exercise on blood flow hemodynamics including the change of flow  
57 patterns across the aortic valve, vorticity, shear rate, stress and strain on the leaflets while  
58 exercise [28]. In our previous studies pressures across the aorta were measured and  
59 applied to models. However, accurate predictions of aortic pressures are only possible using  
60 invasive techniques. Numerical calculation method is a useful tool for prediction of the real  
61 pressure values and it can be used to analyze how different parameters, such as material  
62 properties, affect output. It also has a potential role in clinical diagnosis.

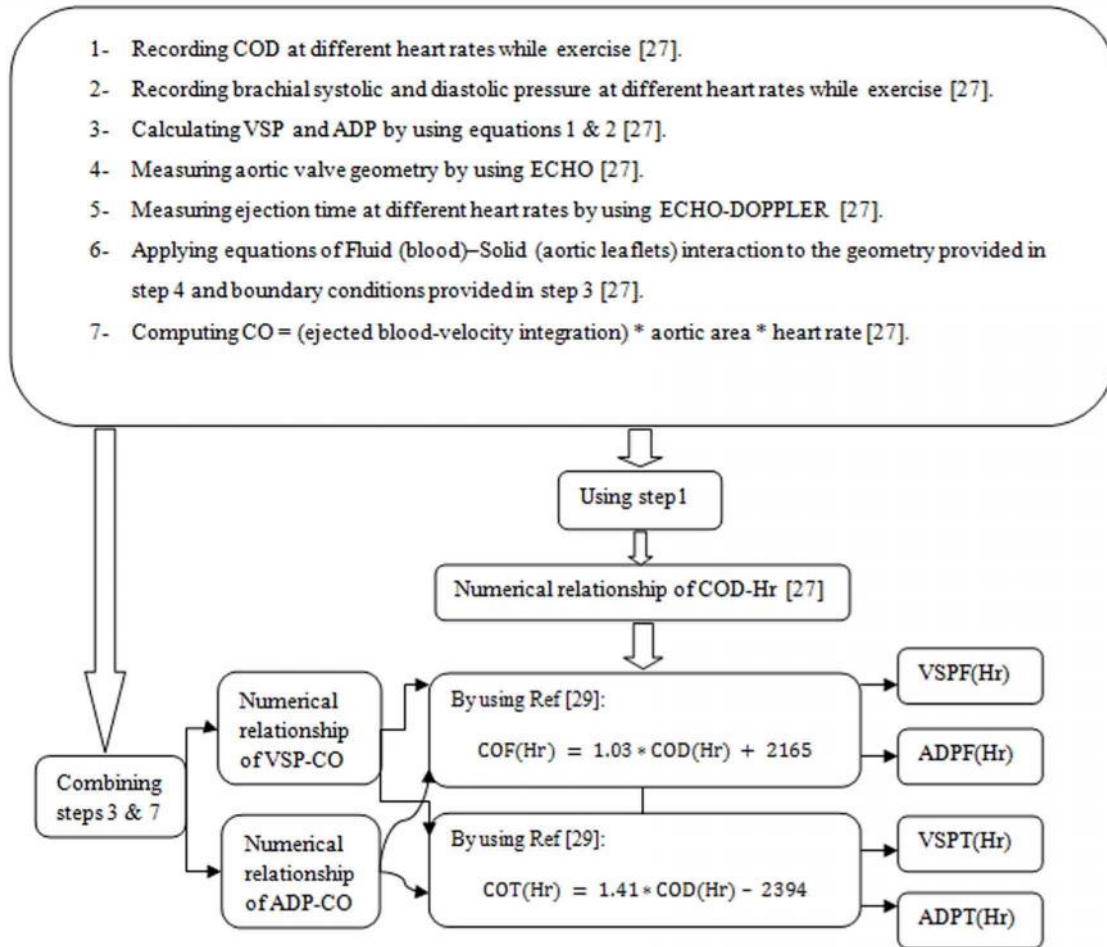
63 The purpose of this study is to predict MPLV (mmHg) by numerical derivation from the  
64 relationship of cardiac output to MPLV (mmHg) [27] from invasive clinical cardiac output  
65 measurement [29]. First, the relationship between cardiac output and systolic ventricular  
66 pressure and systolic aortic pressure is derived, based on a previous numerical study [27].  
67 Additionally, Christie et al.[29] clinically obtained equations for Thermodilution cardiac  
68 output (COT in ml/min) and Fick oximetric cardiac output (COF in ml/min) to Doppler cardiac  
69 output (COD in ml/min). Therefore, COT and COF were measured for the subject [27].  
70 Then, MPLV (mmHg) was calculated noting to the numerical relationship among cardiac  
71 output, systolic ventricular pressure and systolic aortic pressure.

72

## 73 2. MATERIAL AND METHODS

### 74 2.1 Overview

75 We have presented our two-dimensional FSI aortic valve model previously [27 , 28 ]. The  
 76 model, as well as clinical measurements, are briefly described in section 2.2. Section 2.3  
 77 presents the methods to calculate pressure predictions based on cardiac output. **Figure 1**  
 78 **shows the workflow diagram.**



79 **Figure 1.** Workflow diagram.  
 80

81  
 82 **2.2 Combined clinical and numerical approach**

83 A healthy male, aged 33, with normal cardiovascular function had his hemodynamic data  
 84 recorded while at rest and during exercise. Informed consent was acquired for the participant  
 85 in line with accepted procedures approved by the Department of Cardiovascular Imaging  
 86 (Atherosclerosis research center, Tehran, Iran). Hemodynamic data was assessed from  
 87 maximal bicycle exercise tests and Doppler echo. Systolic and diastolic pressures of the  
 88 brachial artery were measured and related to heart rate changes at rest and during exercise  
 89 (Figure 2). Equations 1 and 2 were used to determine the central aortic pressure from  
 90 brachial aortic pressure measurements. This relationship was previously determined by  
 91 comparing brachial pressure (acquired by Oscillometry) to the central pressure acquired  
 92 using an invasive method [30 ].

93  $Central\ systolic\ pressure \approx Brachial\ systolic\ pressure + 2.25$  (1)

94  $Central\ diastolic\ pressure \approx Brachial\ diastolic\ pressure - 5.45$  (2)

95 where all pressures were measured in mmHg.

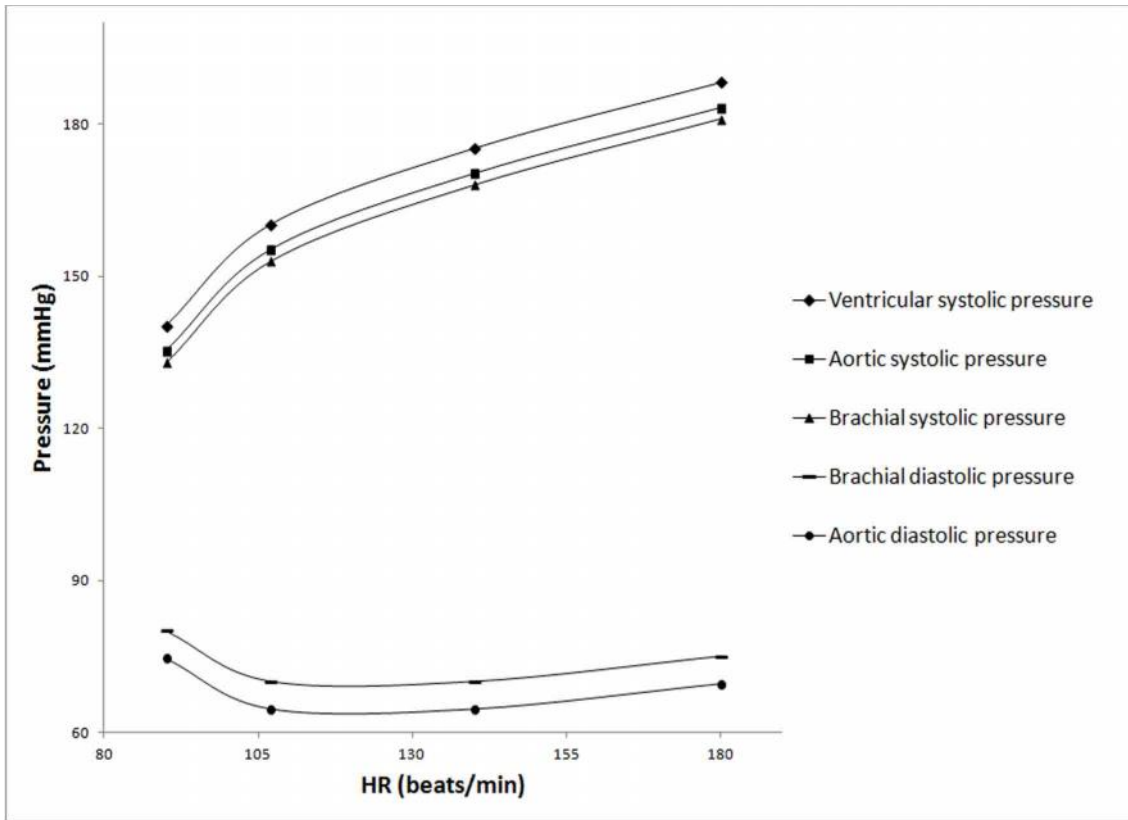


Figure 2. Interpolated curves for brachial, aortic and ventricular pressures.

96  
97  
98  
99  
100  
101  
102  
103  
104

Left ventricular systolic pressure was derived from the calculated central systolic pressure. Previously, a pressure difference of around 5 mmHg was found between peak left ventricular systolic pressure and central systolic pressure, using catheterization [31]. The ejection times were derived from Doppler-flow imaging under B-mode.

Table 1. Geometric parameters of the aortic valve as shown in figure 2.

(a)	(b)	(c)	(d)	(e)	(f)	(g)
Ascending aorta radius after sinotubular junction (mm)	Aortic side radius (mm)	Leaflet's thickness (mm)	Valve's height (mm)	Leaflet's length (mm)	Ventricular side radius (mm)	Maximum radius of normal aortic root (mm)
11.75	11.5	0.6	20.36	16.6	11.1	16.65

105  
106  
107

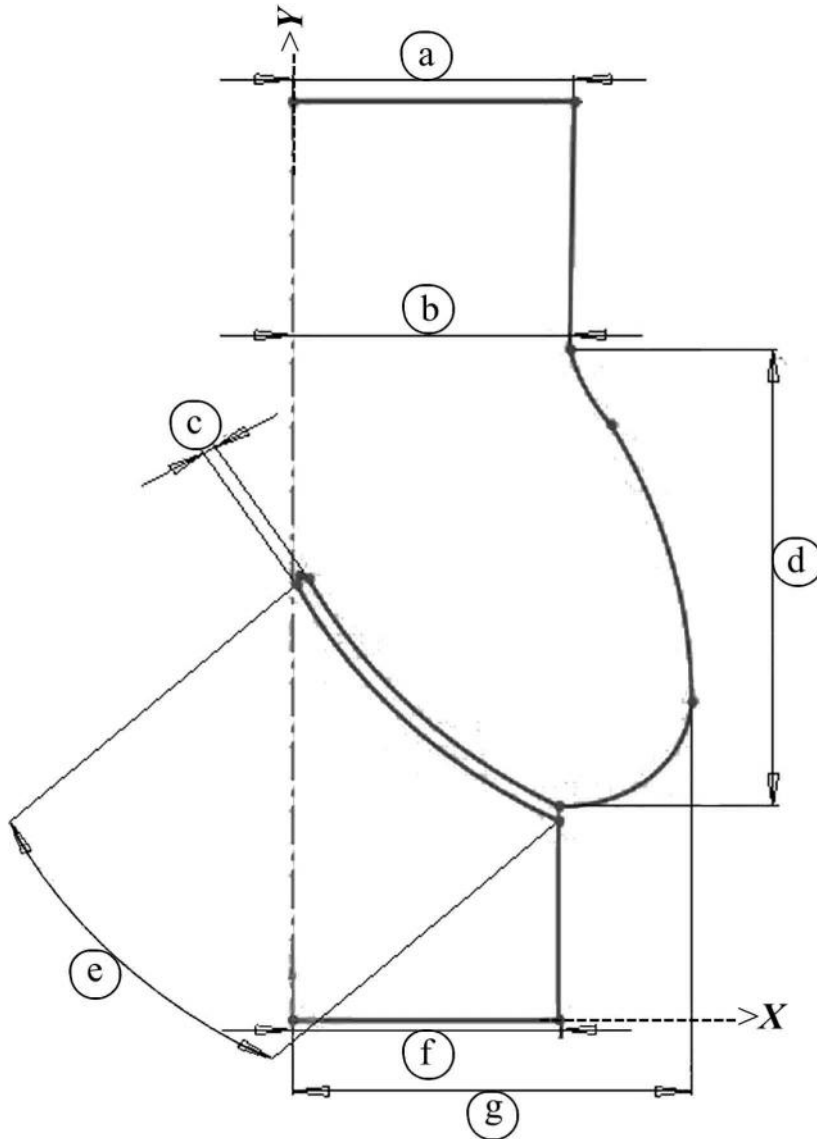
Table 2. Mechanical properties.

Viscosity (Pa.s)	Density (kg/m <sup>3</sup> )	Young's modulus (N/m <sup>2</sup> )	Poisson ratio
3.5 x 10 <sup>-3</sup>	1056	6.885 x 10 <sup>6</sup>	0.4999

108  
109  
110  
111  
112

The aortic valve geometry simulated is presented in figure 3 and dimensions are provided in table 1. Briefly, dimensions were obtained with respect to T-wave of ECG (maximum opening area), with diameters of the aortic valve annulus and the sinus valsalva (the sinus of Valsalva refers to each aortic sinus) measured at the peak T-wave time using a

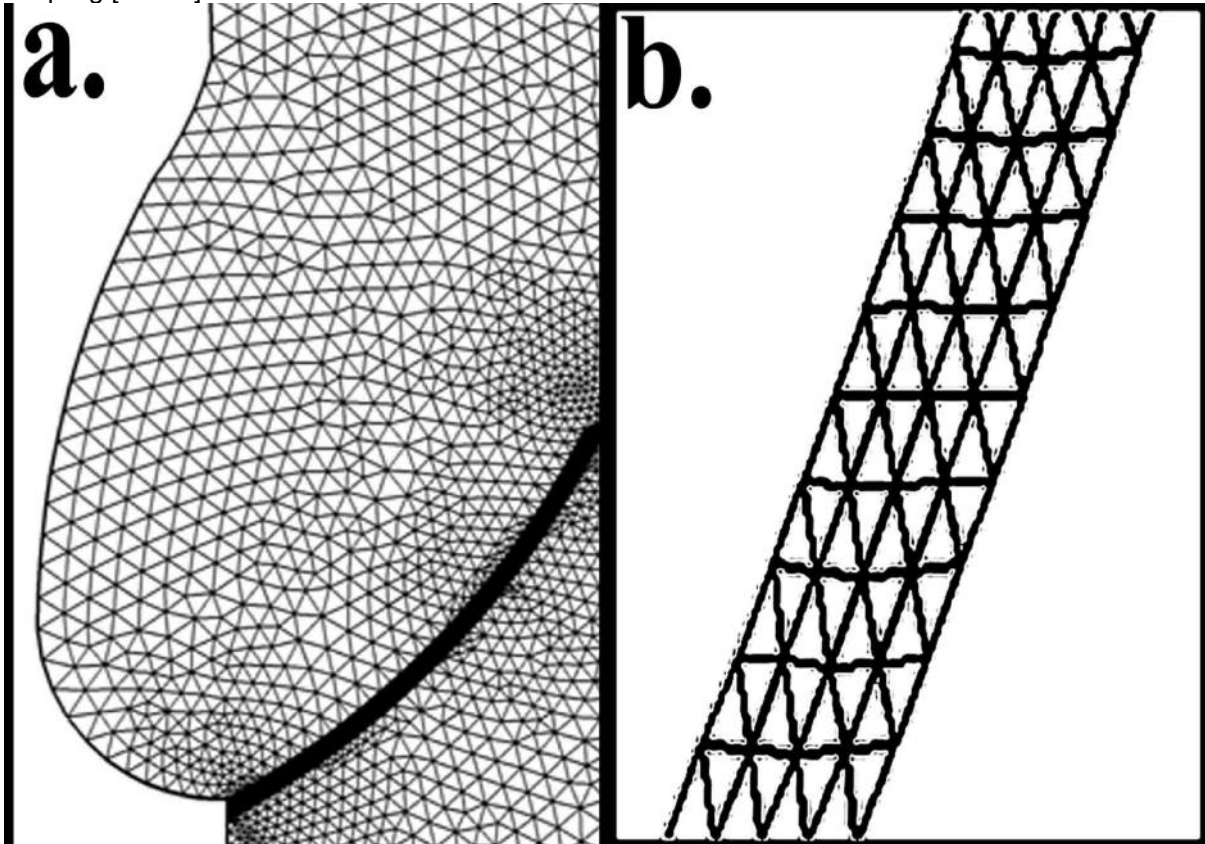
113 resting **parasternal** long-axis view. The two cusps were considered to be isotropic,  
114 homogenous and to have a linear stress-strain relationship. This assumption has been used  
115 in other heart valve models [20 , 23 , 24 , 32 ]. Blood was assumed to be an incompressible  
116 and a Newtonian fluid [16 ]. All material properties are provided in table 2 and were obtained  
117 from the literature [33 , 34 ].



118 **Figure 3.** a) Ascending aorta radial after sinotubular site; b) Aortic side radial; c) Leaflet  
119 thickness; d) Valve height; e) Leaflet length; f) Ventricular side radial; g) Maximum radial of  
120 normal aortic root.  
121  
122

123 For fluid boundaries (figure 3), pressure was applied at the inflow boundary of the aortic root  
124 at the left ventricular side. A moving ALE mesh was used which enabled the deformation of  
125 the fluid mesh to be tracked without the need for re-meshing [35 ]. Second order Lagrangian  
126 elements were used to define the mesh. Two-dimensional triangular planar strain elements  
127 were applied to define the mesh. The mesh contained a total of 7001 elements (Figures 4a  
128 and 4b). The finite element analysis package Comsol Multi-physics (v4.2) [36] was used to

129 solve the FSI model under time dependent conditions [23 , 24 ]. The fluid velocity is coupled  
 130 to the structural deformation while the valve is loaded by the fluid, this ensures simultaneous  
 131 coupling [37-40 ].



132 **Figure 4. Meshes for the (a) the fluid domain and (b) the solid domain.**

### 136 2.3 Cardiac measurements

137 Regression equations were used to calculate left ventricular systolic pressure (VSP (mmHg);  
 138 equation 3) and aortic diastolic pressure (ADP (mmHg); equation 4) from the cardiac output  
 139 predicted numerically (figure 5). :

$$140 \text{VSP} = 1.266\text{E} - 06 * (\text{CO})^2 - 0.017 * (\text{CO}) + 152.3 ; (R^2=0.997) \quad (3)$$

$$141 \text{ADP} = 5.915\text{E} - 07 * (\text{CO})^2 - 0.014 * (\text{CO}) + 142.2 ; (R^2=0.965) \quad (4)$$

142 Please note that E refers to exponent.

143 Previously we extracted the relationship between Doppler cardiac output and heart rate  
 144 (beat/min) using equation 5 [27]:

$$145 \text{COD} = -0.498 * (\text{Hr})^2 + 213.550 * (\text{Hr}) - 6164 ; (R^2 = 0.995) \quad (5)$$

146 Christie et al. [29] obtained regression equations for the relationships between  
 147 Thermodilution cardiac output (COT (ml/min)) and Fick oximetric cardiac output (COF  
 148 (ml/min)) to Doppler cardiac output (COD (ml/min)), based on the data given from 15  
 149 subjects:

$$150 \text{COT} = 1.41 * \text{COD} - 2394 \quad (6)$$

$$151 \text{COF} = 1.03 * \text{COD} + 2165 \quad (7)$$

152 Combining equations (6) and (7) with equation (5) by applying Matlab (MATLAB version  
 153 7.10.0, Natick, Massachusetts, The MathWorks Inc, 2010.), we have extracted the following

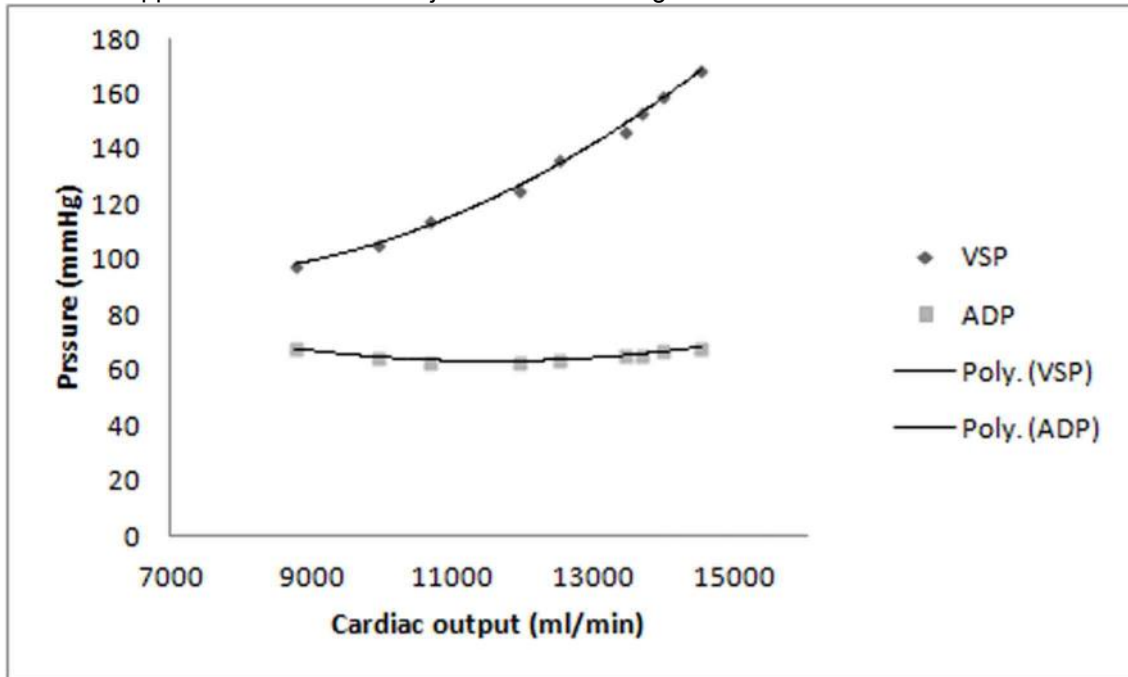
154 relations and shown the curves of Fick oximetric (COF (ml/min)) and Thermodilution  
155 cardiac output (COF (ml/min)) relative to the heart rate in Figure 6.

156  $COF = -0.705 * (Hr)^2 + 301.796 * (Hr) - 11131;$  (8)

157  $COF = -0.515 * (Hr)^2 + 220.461 * (Hr) - 4217;$  (9)

158

159 Combining equations (3) and (4) with equation (8), enables VSP and ADP to be plotted with  
160 respect to heart rate respectively, based on Thermodilution method. These plots are shown  
161 in figures 7 and 8. Also, Combining equations (3) and (4) with equation (9) enables us to plot  
162 VSP and ADP with heart rate, respectively. The plots derived from a Fick oximetric method  
163 are shown in figures 7 and 8. Combining equations (3) and (4) with equation (5), enables the  
164 plotting of VSP and ADP with respect to heart rate, respectively. The plots derived from the  
165 use of a Doppler method for our subject are shown in figures 7 and 8.



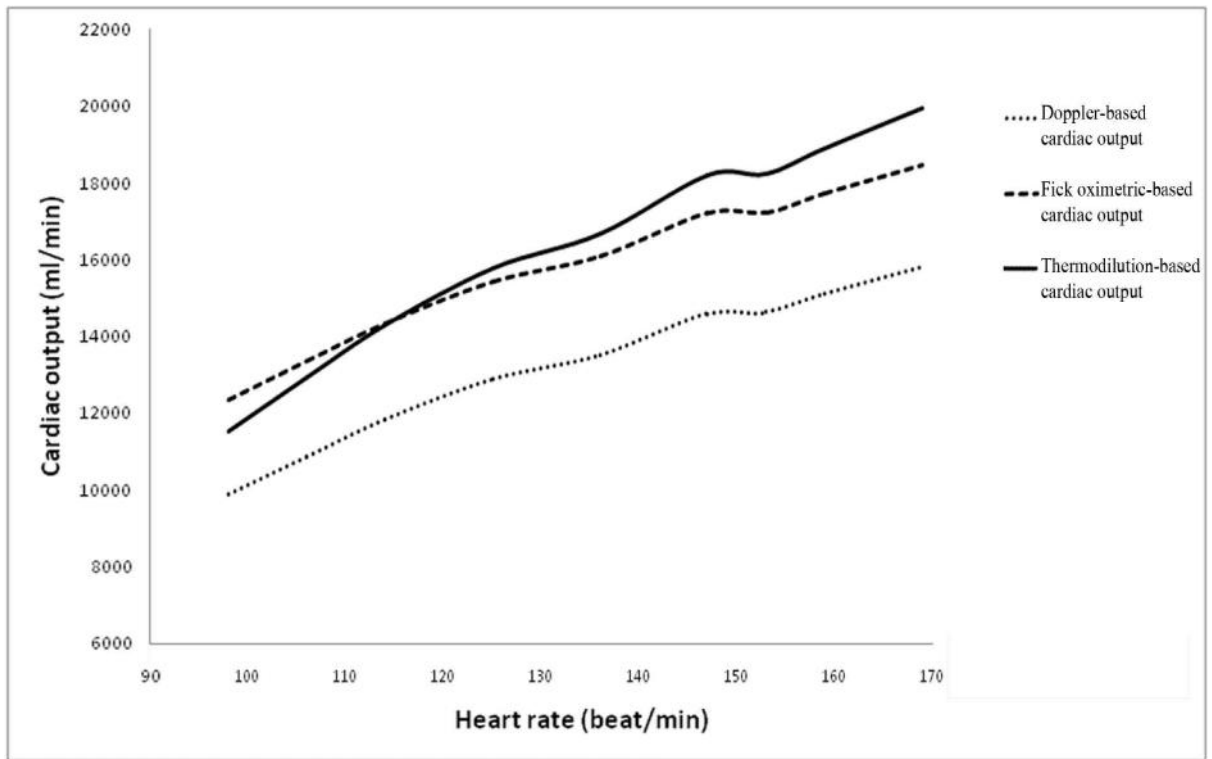
166

167

168 **Figure 5.** Ventricular systolic pressure (VSP) and Aortic diastolic pressure (ADP) to cardiac  
169 output that were plotted for numerical method.

170

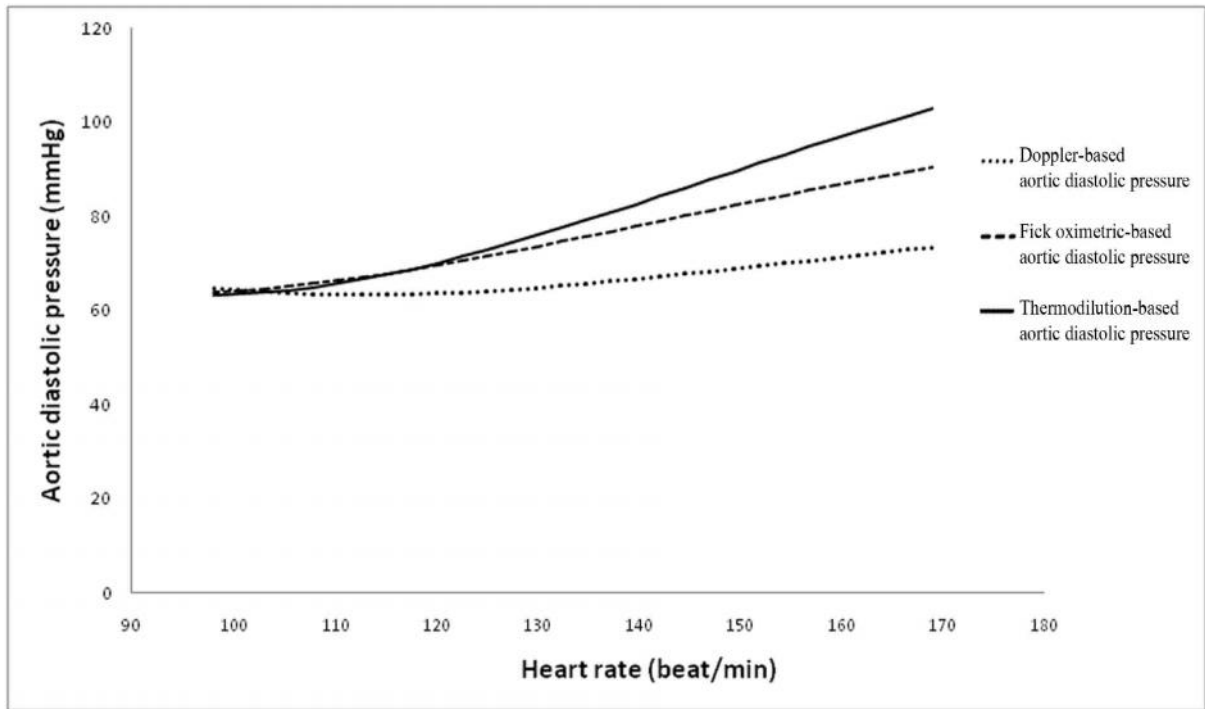
171  
172



173  
174  
175  
176  
177  
178

**Figure 6.** FSI prediction of cardiac output's change relative to heart rate based on Doppler method (round dot line), Fick oximetric method (square dot line), Thermodilution method (solid line).

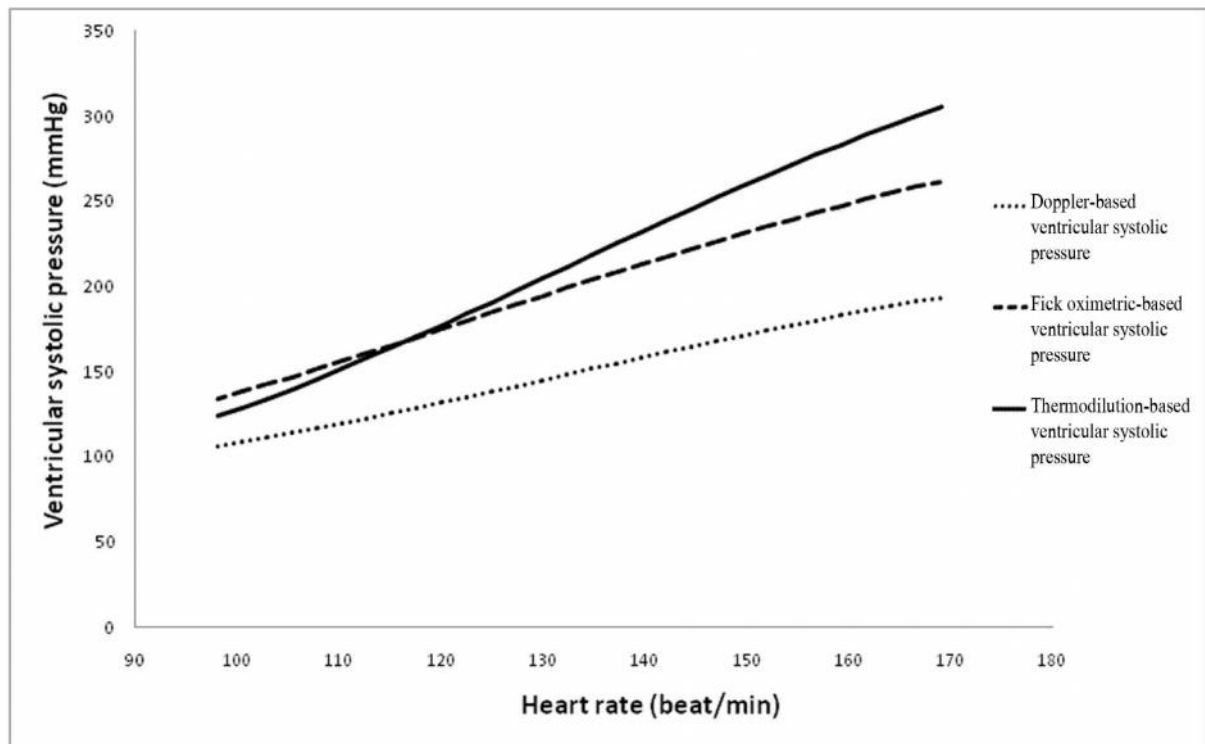
179  
180



181  
182  
183  
184  
185  
186

**Figure 7.** FSI prediction of aortic diastolic pressure's change relative to heart rate based on Doppler method (round dot line), Fick oximetric method (square dot line), Thermodilution method (solid line).

187  
188



189  
190 **Figure 8.** FSI prediction of ventricular systolic pressure's change relative to heart rate based  
191 on Doppler method (round dot line), Fick oximetric method (square dot line), Thermodilution  
192 method (solid line).  
193

194

### 195 3. RESULTS

196 Aortic diastolic pressure, derived from Doppler based measurements, increased by 13.4%,  
197 corresponding to 8.7 mmHg, with increasing heart rate from 98 bpm to 169 bpm. Instead,  
198 using the Fick oximetric method there was a 42% increase corresponding to 26.7 mmHg.  
199 Whereas thermodilution led to a prediction of a 62.6% increase, corresponding to 39.6  
200 mmHg. The mean slopes obtained from curves of aortic diastolic pressure based on  
201 Doppler, Fick oximetric and thermodilution methods were 0.14, 0.40 and 0.60 (mmHg\*min),  
202 respectively.

203 The ventricular systolic pressure, predicted from the Doppler method, increased 82.1%,  
204 corresponding to 87.2 mmHg, with increasing heart rate from 98 bpm to 169 bpm (figure 8).  
205 This increase was calculated to be 95.6%, corresponding to 127.9 mmHg, using the Fick  
206 oximetric method and 147% (or 181.6 mmHg) for the Thermodilution method. The mean  
207 slopes obtained from curves of ventricular systolic pressure based on Doppler, Fick  
208 oximetric and Thermodilution methods are 1.27, 1.85 and 2.65 (mmHg/heart rate),  
209 respectively.  
210

### 211 4. DISCUSSION

212  
213

#### 213 4.1 Study findings

214 The study has combined FSI hemodynamic measurements of the cardiac output, from a  
215 healthy subject [27] with invasive clinical measurements [29] in order to estimate the  
216 maximum pressure in the left ventricles during exercise. Based on the author's current

217 knowledge, two-dimensional FSI discipline has been integrated with exercise measurements  
218 to numerically predict of cardiovascular performance for the first time. Despite using a  
219 simplified two-dimensional model, the method developed has potential for clinical application  
220 (section 4.2) and the obtained values show good agreement with the literature (see section  
221 4.3). Moreover, the FSI model predicted MPLV over a range of heart rates based on clinical  
222 measurement of cardiac outputs. MPLV was calculated by cardiac output of Doppler  
223 method, Fick oximetric and thermodilution method which shows 82.1%, 95.6% and 147%  
224 increment during exercise. Our predicted Fick-MPLV values were 8% to 19% lower ,  
225 Thermodilution-MPLV lower by 17% to 25% ,and Doppler-MPLV 57% to 73% lower than  
226 Doppler methods (Please see section 4.3 Comparison to literature) So, our predicted Fick-  
227 MPLV values are probably accurate to within 81% to 92%, Thermodilution-MPLV ones 75%  
228 to 83% ,and Doppler-MPLV ones 27% to 43% when compared to clinical reports.  
229 Since cardiac output calculated with Fick method eliminates the plights associated with  
230 measuring VO<sub>2</sub> precisely and do not require either an assumption of or measurement of the  
231 respiratory exchange ratio, that may prove to be more clinically useful for continuous cardiac  
232 output monitoring than Thermodilution cardiac [41, 42]. In this regard we can say that our  
233 Fick-based results could be more precise than the other two methods. Christie et al,  
234 furthermore, reported the advantage of Doppler measurement is its operational feasibility,  
235 although its outputs can be modified by the correlation equations between that and invasive  
236 techniques [29 ].  
237 The mean slopes derived from curves, shown in fig 8, of VSP, are 1.27 (Doppler-based),  
238 1.85 (Fick-based) and 2.65 (Thermodilution-based) (mmHg\*min).

#### 240 **4.2 Clinical application & reliability**

241 Predicting reliable intraventricular pressures is important in clinical diagnosis and treatment  
242 [2]. For instance, one of the recent commercially available medical investigating devices to  
243 assess intraventricular pressure has a fluid-filled, balloon-tipped catheter that is intended for  
244 insertion into the ventricle [14]. The balloon provides a closed system from which  
245 intraventricular pressure is determined. The balloon is attached to a fluid-filled catheter and  
246 connected to a pressure transducer and bridge amplifier [14]. This highly advanced method  
247 clearly demonstrates its involved risk and because of that they are mostly applicable for  
248 animal studies due to their invasive method.  
249 The presented non invasive method lets us predict more accurate MPLV by measuring  
250 brachial pressures of subjects. Our numerical estimations based on Fick oximetric have  
251 potential for clinical application (8% to 19% underestimation when compared to clinical  
252 approaches; see discussion, Comparison to literature), this is important because Fick  
253 methods' evaluations have been reported to be more accurate than other clinical  
254 approaches [41, 42, 43, 44]. Catheterization-thermodilution , the current gold-standard for  
255 measuring intraventricular pressure [4], is an invasive procedure with potential risks such as  
256 heart failure, cardiac arrhythmia, and even death [4]. Moreover, thermodilution sometimes  
257 exposes the patient and doctor to radiation. Exercising while catheterized results in a range  
258 of practical problems too, therefore, is not common customary action. However, the use of a  
259 numerical method permits the estimation of cardiac function by non-invasive measurements  
260 during an exercise protocol. Therefore, the key-concern is the dependability of numerical  
261 methods when predicting MPLV while exercise. Yet, computational methods have not been  
262 combined with non-invasive clinical measurements to predict a patient's MPLV. Our model  
263 enables assessment of cardiac function and hemodynamic changes from rest to exercise [27  
264 , 28 ]. It was feasible to derive the relationship for cardiac output to MPLV. Concerning  
265 invasive clinical cardiac output measurement as more accurate [29 ], we are able to estimate  
266 more precise MPLV. It should also be mentioned that most of clinical measurement of MPLV  
267 have done for animals like dog such as the Monroe study [45] due to the risk associated with  
268 them.

269 It is generally accepted that cardiovascular modelling is a mechanical-based system, in  
270 particular when the mechanical characteristic (e.g. MPLV) is intended to investigate. In this  
271 point of view, development of such mechanical simulations can be resulted in more accurate  
272 prediction of cardiovascular performance. By this it is thought that electrical-based  
273 simulations are more limited and less useful as compared to mechanical-based modelling.  
274 Based on our current knowledge, the maximum pressure of left ventricle, for example, has  
275 not been studied yet by electrical-based modelling.  
276

### 277 **4.3 Comparison to literature**

278 Following a literature search we have not found a previous comparable study that combined  
279 a clinical and numerical approach to predict MPLV during exercise. In our study, the patient  
280 specific MPLV were predicted at a range of heart rates induced by exercise for echo-  
281 Doppler, thermodilution, and Fick oximetric methods. While the variation for MPLV from rest  
282 to peak of external work is established [3] this is the first study to use numerical methods to  
283 predict these values for an individual. Textbook MPLV range from 80 (mmHg) at 70 bpm to  
284 270 mmHg at 180 bpm. It could also be approximated that the slope of MPLV is about 2.2  
285 mmHg\*min for non athletes during exercise [3]. Our subject is also a nonathlete. Our  
286 thermodilution-based prediction is overestimated by 17%, our Fick oximetric-based  
287 prediction is underestimated by 19% and our Doppler prediction is underestimated by 73%  
288 when compared to textbook values.

289 Loeppky et al. clinically investigated the systolic blood pressure changes while exercise for  
290 ten subjects. The mean slope of MPLV over the exercise protocol roughly was 2 mmHg\*min  
291 [46]. Our thermodilution-based estimation is overestimated by 25%, our Fick oximetric-based  
292 estimations is underestimated by 8% and our Doppler-based estimation is underestimated  
293 by 57% when compared to the results from Loeppky et al.

294 Compared to published values [3, 46], our results based on thermodilution method are  
295 overestimated by 17% to 25%, the Fick oximetric method underestimates values by 8% to  
296 19% and the Doppler method leads to underestimates of 57% to 73% when compared to  
297 clinical data.

298 Fick methods' evaluations has been reported to be more accurate [41, 42]. Hence, our  
299 numerical estimations based on Fick oximetric are more reliable when it is considered that  
300 an 8% to 19% underestimation could be due to our considered limitations for the numerical  
301 model or that only single subject was investigated. Textbook maximum systolic pressure for  
302 the normal left ventricle range from 250 to 300 mmHg, but varies widely among different  
303 subjects with heart strength and degree of heart stimulation by cardiac nerves. [10] MPLV  
304 has been studied by catheterization. MPLV ranged between 121 (mmHg) at the heart rate of  
305 75 bpm to 210 (mmHg) at 180 bpm. They reported the average of MPLV of 6 patients with  
306 normal left ventricular function and no valve abnormalities, was 121 (mmHg) at 75 bpm at  
307 rest to 149 (mmHg) at 108 bpm during exercise. Although our study is numerical and based  
308 on one subject, our model predicted MPLV would be useful to quantify how closely the  
309 values match the literature.

310

### 311 **4.4 Limitations & future trends**

312 A fully developed discussion of the limitations of the FSI model has been explained  
313 previously [27]. In short, the main limitations are that:

- 314 ▪ there are simplifications of the mechanical properties, plus using a constant orifice  
315 area and a single diameter for the ascending aorta in the model;
- 316 ▪ statistical and generalized data was applied for clinical determination of  
317 hemodynamic;
- 318 ▪ Instead of three-dimensional structure a two-dimensional model was used to  
319 investigate;

320     ▪     The model was performed for a healthy subject. However, it should be noted that  
321     patients with cardiopathies may present different hemodynamic and structural  
322     alterations.

323     ▪     The study presents a nearly perfect quadratic relation between cardiac output and  
324     heart rate. And this is the results of comparing just these two parameters. Although  
325     some factors like preload, afterload and cardiac contractility should be considered as  
326     other elements at the future study. This should be noted that our subject was  
327     examined at the condition lack of preload, afterload and cardiac contractility.

328     Despite model limitations we previously presented excellent agreement with clinical  
329     measurements and the general literature [27 ]. A real model as three-dimensional could  
330     results more precise predictions, while, it would also increase the solution time (currently  
331     less than 15 minutes). This would hold disadvantages for clinical applications, yet, it is  
332     required to be balanced against the short solution time for a 2D FSI model. Our model  
333     solution time is potentially able to be translated into clinical **practice**; moreover, ameliorating  
334     of solution time can be possible with more robust computer power. Furthermore, a range of  
335     values for statistical comparison are not predictable without the including variability in  
336     models [24 ]. At this time, there is a tendency towards patient specific models, like [47 ], due  
337     to potential profits in aiding treatment/diagnosis for an individual. Prediction of  
338     intraventricular pressure could be useful to construct more reliable heart valve prototypes  
339     [48].

340     Although **the** patterns **of** pressure of left ventricle **are** imposed by its walls contraction, we  
341     predicted this with comparing the underestimated numerical values of cardiac output [27 ]  
342     with that of invasive clinical reports [29 ]. Needless to say, this underestimation resulted from  
343     pressures of boundary conditions. Consequently, they were studied to be modified to  
344     correspond with clinical approaches.

345     A 2D model allows us to calculate quickly, in comparison with the 3D model. However,  
346     validation was done for that [27]. MPLV is the crucial contributor as the boundary condition in  
347     the aortic valve motions. To gain more exact result, clearly we must use the mechanism of  
348     aortic valve associated with the MPLV.

349     MPLV is the result of mechanical-based equation involved with the sophisticated aortic valve  
350     geometry. Thus, our mechanical model working on the mechanical relationship (FSI), are  
351     probable to result in more reasonable data. The rate of assumption is so high in the electrical  
352     model. Unlike electrical ones, our mechanical model can provide you mechanical  
353     parameters at each point of (x,y,z) that would be useful for further investigation.

354

#### 355     **4. CONCLUSION**

356

357     We introduced a two-dimensional model of aortic valve which is able to predict maximum  
358     pressure in the left ventricles during exercise using **FSI**. The model was analyzed against  
359     results from echo-Doppler, thermodilution and Fick oximetric methods as invasive and non-  
360     invasive clinical methods. The model has potential applications in the prediction of  
361     ventricular pressures. As clinical Fick-measured values have been suggested as most  
362     accurate, our Fick-based predictions are likely the most applicable. **The credibility and**  
363     **preciseness of this numerical technique for clinical application with human subjects would**  
364     **require further appropriate clinical studies.**

365

## 5. Abbreviations

Term	Description
MPLV	Maximum pressure in the left ventricle
ALE	Arbitrary Lagrangian-Eulerian
FSI	Fluid-structure interaction
COT	Thermodilution cardiac output
COF	Fick oximetric cardiac output
COD	Doppler cardiac output
VSP	ventricular systolic pressure
ADP	Aortic diastolic pressure
ADPD	FSI prediction of aortic diastolic pressure's change relative to heart rate based on Doppler method
ADPF	FSI prediction of aortic diastolic pressure's change relative to heart rate based on Fick oximetric method
ADPT	FSI prediction of aortic diastolic pressure's change relative to heart rate based on Thermodilution method
VSPD	FSI prediction of ventricular systolic pressure's change relative to heart rate based on Doppler method
VSPF	FSI prediction of ventricular systolic pressure's change relative to heart rate based on Fick oximetric method
VSPT	FSI prediction of ventricular systolic pressure's change relative to heart rate based on Thermodilution method

367

368

369

## COMPETING INTERESTS

370

The authors of the manuscript declare that they have no conflict of interest.

372

373

## REFERENCES

374

375

1. Murphy SL, Xu J: Deaths: Preliminary Data for 2010, National Vital Statistics Reports 2012 4(60):31, 2010.

376

377

2. Bonow RO, Mann DL, Zipes DP, Libby P, Book Braunwald's Heart Disease: A Textbook of Cardiovascular Medicine 9th ed, Philadelphia, Pa: Saunders Elsevier 2011.

378

379

3. Guyton. AC, Hall JE, Textbook of Medical Physiology, Philadelphia PA, WB Saunders P:27, 1996.

380

381

4. Lavdaniti M, , *Int J Caring Sci* 1(3):112–117, 2008.

382

383

5. Courtois MA, Kovacs SJ, Ludbrook PA, Physiologic early diastolic intraventricular pressure gradient is lost during acute myocardial ischemia, *Circulation* 82:1413–23, 1990.

384

385

6. Brenner JI, Baker KR, Berman MA: Prediction of left ventricular pressure in infants with aortic stenosis. *Br Heart J* 44(4):406-10, 1980.

386

387

7. Greenberg NL, Vandervoort PM, Thomas JD, Instantaneous diastolic transmitral pressure differences from color Doppler M mode echocardiography, *Am J Physiol* 271:H1267–76, 1996.

388

389

8. Firstenberg MS, Vandervoort PM, Greenberg NL, et al, Noninvasive estimation of transmitral pressure drop across the normal mitral valve in humans: importance of

390

391

392

- 393 convective and inertial forces during left ventricular filling, *J Am Coll Cardiol*  
394 36:1942–9, 2000.
- 395 9. Tonti G, Pedrizzetti G, Trambaiolo P, Salustri A, Space and time dependency of  
396 inertial and convective contribution to the transmitral pressure drop during  
397 ventricular filling, *J Am Coll Cardiol* 38:290–1, 2001.
- 398 10. Pasipoularides A, Murgo JP, Miller JW, Craig WE, Nonobstructive left ventricular  
399 ejection pressure gradients in man, *Circ Res* 61(2):220-7, 1987.
- 400 11 Redaelli A, and Montevecchi FM, Computational evaluation of intraventricular  
401 pressure gradients based on a fluid-structure approach, *Journal of Biomechanical*  
402 *Engineering, transactions of the ASME* 118 (4): 529–537, 1996.
- 403 12. Clavin OE, Spinelli JC, Alonso H, Solarz P, Valentinuzzi ME, Pichel RH, Left  
404 intraventricular pressure–impedance diagrams (DPZ) to assess cardiac function.  
405 Part I: morphology and potential sources of artifacts, *Med Progn Technol* 11: 17–24,  
406 1986.
- 407 13. Spinelli JC, Clavin OE, Cabrera EI, Chatruc MR, Pichel RH, Valentinuzzi ME, Left  
408 intraventricular pressure–impedance diagrams (DPZ) to assess cardiac function.  
409 Part II: determination of end-systolic loci. *Med Progn Technol* 11: 25–32, 1986.
- 410 14. Sutherland, Fiona J, et al. Mouse isolated perfused heart: characteristics and  
411 cautions. *Clinical and experimental pharmacology and physiology* 30.11 (2003):  
412 867-878.
- 413 15 . Bellhouse BJ, The fluid mechanics of heart valves. In: Book Cardiovascular fluid  
414 mechanics, Volume 1, Bergel DH (ed), London Academic Press, 1972.
- 415 16 . Caro CG, Pedley TJ, Schroter RC, Seed WA, Book The mechanics of the  
416 circulation, Oxford: Oxford University Press, 1978.
- 417 17 . Donea J, Giuliani S, Halleux JP, An arbitrary Lagrangian–Eulerian finite element  
418 method for transient dynamic fluid–structure interactions, *Comput Methods Appl*  
419 *Mech Engrg* 33(1-3):689 –723, 1982.
- 420 18 . Formaggia L, Nobile F, A stability analysis for the arbitrary Lagrangian Eulerian  
421 formulation with finite elements, *East–West J Numer Math*7(2):105–132, 1999.
- 422 19 . Al-Atabi M, Espino DM, Hukins DWL, Computer and experimental modelling of  
423 blood flow through the mitral valve of the heart, *J Biomech Sci Eng* 5(1):78-84, 2010.
- 424 20 . De Hart J, Peters GW, Schreurs PJ, Baaijens FP, A two-dimensional fluid-structure  
425 interaction model of the aortic valve, *J Biomech* 33(9):1079-1088, 2000.
- 426 21 . De Hart J, Peters GW, Schreurs PJ, Baaijens FP, A three-dimensional  
427 computational analysis of fluid–structure interaction in the aortic valve, *J Biomech*  
428 36(1):103-112, 2003a.
- 429 22 . De Hart J, Baaijens FP, Peters GW, Schreurs PJ, A computational fluid-structure  
430 interaction analysis of a fiber-reinforced stentless aortic valve, *J Biomech* 36(5):699-  
431 712, 2003b.
- 432 23 . Espino DM, Shepherd DET, Hukins DWL, Evaluation of a transient, simultaneous,  
433 Arbitrary Lagrange Euler based multi-physics method for simulating the mitral heart  
434 valve, *Comput Methods Biomech Biomed Engin* In Press. DOI:  
435 10.1080/10255842.2012.688818, 2012a.
- 436 24 . Espino DM, Shepherd DET, Hukins DWL, A simple method for contact modelling in  
437 an arbitrary frame of reference within multiphysics software, *J Mech*, In Press DOI:  
438 10.1017/jmech.2012.128 , 2012b.
- 439 25 . Stijnen JMA, De Hart J, Bovendeerd PHM, Van de Vosse FN, Evaluation of a  
440 fictitious domain method for predicting dynamic response of mechanical heart  
441 valves, *J Fluids Struct* 19(6):835-850, 2004.
- 442 26 . Xia .G.H, Zhao .Y and Yeo .J.H , Numerical Simulation of 3D Fluid-Structure  
443 Interaction Using AN Immersed Membrane Method, *Modern Physics Letters B*  
444 19(28-29):1447-1450. 2005

- 445 27 . Bahraseman HG, Hassani K, Navidbakhsh M, Espino DM, Sani ZA, Fatourae N,  
446 Effect of exercise on blood flow through the aortic valve: a combined clinical and  
447 numerical study. *Comput Methods Biomech Biomed Engin*, In Press. DOI:  
448 10.1080/10255842.2013.771179, 2013.
- 449 28 . Bahraseman HG, Hassani K, Navidbakhsh M, Espino DM, Fatourae N, Combining  
450 numerical and clinical methods to assess aortic valve hemodynamics during  
451 exercise, *Journal of perfusion*, Accepted in 1/3/2014 & is in press.
- 452 29 . Christie J, Sheldahl LM, Tristani FE, Sagar KB, Ptacin MJ, Wann S, Determination  
453 of stroke volume and cardiac output during exercise: comparison of two-dimensional  
454 and Doppler echocardiography, Fick oximetry, and Thermodilution , *Circulation*  
455 76(3):539-547, 1987.
- 456 30 . Park SH, Lee SJ, Kim JY, Kim MJ, Lee JY, Cho AR, Lee HG, Lee SW, Shin WY, Jin  
457 DK, Direct Comparison between Brachial Pressure Obtained by Oscillometric  
458 Method and Central Pressure Using Invasive Method, *Soonchunhyang Medical*  
459 *Science* 17(2):65-71, 2011.
- 460 31 . Laske A, Jenni R, Maloigne M, Vassalli G, Bertel O, Turina MI, Pressure gradients  
461 across bileaflet aortic valves by direct measurement and echocardiography, *Ann*  
462 *Thorac Surg* 61(1):48-57, 1996.
- 463 32 . Weinberg EJ, Kaazempur-Mofrad MR, A multiscale computational comparison of  
464 the bicuspid and tricuspid aortic valves in relation to calcific aortic stenosis, *J*  
465 *Biomech* 41(16):3482–3487, 2008.
- 466 33 . Govindarajan V, Udaykumar H.S, Herbertson L.H, Deutsch S, Manning K.B, and  
467 Chandran K.B, Two-Dimensional FSI Simulation of Closing Dynamics of a Tilting  
468 Disk Mechanical Heart Valve, *J. Med. Devices* 4(1): 011001(1-11), 2010.
- 469 34 . Koch TM, Reddy BD, Zilla P, Franz T, Aortic valve leaflet mechanical properties  
470 facilitate diastolic valve function, *Comput Methods Biomech Biomed Engin*  
471 13(2):225-34, 2010.
- 472 35 . Winslow AM, Numerical solution of the quasilinear poisson equation in a nonuniform  
473 triangle mesh, *J Comput Phys* 1(2):149-172, 1966.
- 474 36 . *Cmsol Users Manual. 2011. Cmsol Multiphysics Users Guide. Londen: Cmsol*  
475 *Ltd.*
- 476 37 . Dowell EH, Hall KC, Modelling of fluid-structure interaction, *Annu Rev Fluid Mech*  
477 33(1):445-490, 2001.
- 478 38 . Wall W, Gerstenberger A, Gamnitzer P, Forster C, Ramm E, Large deformation  
479 fluid-structure interaction – advances in ALE methods and new fixed grid  
480 approaches *In: Fluid-structure interaction*, Bungartz HJ, Shafer M (Eds.) Berlin:  
481 Springer, 2006.
- 482 39 . Van de Vosse FN, De Hart J, Van Oijen CHGA, Bessems D, Gunther TWM, Segal  
483 A, Wolters BJBM, Stijnen JMA, Baaijens FPT, Finite-element-based computational  
484 methods for cardiovascular fluid-structure interaction, *J Eng Math* 47(3-4):335–368,  
485 2003.
- 486 40 . Sudharsan NM, Murali K, Kumar K, Finite element analysis of non-linear fluid  
487 structure interaction in hydrodynamics using mixed Lagrangian-Eulerian method.  
488 *International Journal of Computational Engineering Science* 5(02):425-444, 2004.
- 489 41. Mahutte CK, Jaffe MB, Chen PA, Sasse SA, Wong DH, Sassoon CS, Oxygen Fick  
490 and modified carbon dioxide Fick cardiac outputs, *Crit Care Med* 22(1):86-95, 1994.
- 491 42. Jarvis SS, Levine BD, Prisk GK, Shykoff BE, Elliott AR, Rosow E, Blomqvist CG,  
492 Pawelczyk JA, Simultaneous determination of the accuracy and precision of closed-  
493 circuit cardiac output rebreathing techniques, *J Appl Physiol* 103(3):867-74. Epub  
494 2007 Jun 7, 2007.
- 495 43 . Maroni JM, Oelberg DA, Pappagianopoulos P, Boucher CA, Systrom DM, Maximum  
496 Cardiac Output During Incremental Exercise by First-pass Radionuclide  
497 Ventriculography, *Chest* 114(2):457-461, 1998.

- 498  
499  
500  
501  
502  
503  
504  
505  
506  
507  
508  
509  
510  
511  
512  
513  
514  
515  
516
- 44 .Sugawara J, Tanabe T, Miyachi M, Yamamoto K, Takahashi K, Iemitsu M, Otsuki T, Homma S, Maeda S, Ajsaka R, Matsuda M, Non-invasive assessment of cardiac output during exercise in healthy young humans: comparison between Modelflow method and Doppler echocardiography method, *Acta Physiol Scand* 179(4):361–366, 2003.
  - 45 . Monroe RG, La Farge CG, Gamble WJ, Hammond RP, Gamboa R, Left ventricular performance and blood catecholamine levels in the isolated heart, *Am J Physiol* 211(5):124854, 1966.
  46. Loepky JA, Gurney B, Kobayashi Y, Icenogle MV. Effects of ischemic training on leg exercise endurance, *J Rehabil Res Dev* 42(4):511-22, 2005.
  - 47 . Öhman C, Espino DM, Heinmann T, Baleani M, Delingette H, Viceconti M, Subject-specific knee joint model: Design of an experiment to validate a multi-body finite element model, *Visual Comp* 27(2):153-159, 2011.
  48. Janko F Verhey, corresponding author, Nadia S Nathan, Otto Rienhoff, Ron Kikinis, Fabian Rakebrandt, and Michael N D'Ambra, Finite-element-method (FEM) model generation of time-resolved 3D echocardiographic geometry data for mitral-valve volumetry, *Biomed Eng Online* 5: 17. Published online 2006 March 3. doi: 10.1186/1475-925X-5-17, 2006.